SHAPE EFFECTS ON DRAG

K. Gemba
Department of Aerospace Engineering, California State University, Long Beach, California 90840
(Dated: May 17, 2007)

It is well known that an objects shape plays a critical role in the drag produced while subjected to a free stream flow. This experiment was conducted to become more familiar with the effects an object' shape has on drag. Utilizing a single component balance in a subsonic windtunnel, testing was conducted at different flow speeds to measure corresponding drag forces. The four objects were subjected to free stream velocities ranging from $11\frac{m}{s}$ to $22\frac{m}{s}$ with drag forces measurements ranging from 0.6 N to 1.7 N. When each object was subjected to the maximum flow velocity condition ($22\frac{m}{s}$) Objects 1, possessing the largest projected area, exhibited a drag force 2 times greater than that of the most "aerodynamically" shaped object, Object 6. The coefficient of drag and Reynolds numbers were calculated for each object. Object 3 had the largest coefficient of drag values with a maximum value of 4.76. Reynolds numbers were similar for all three objects and ranged from 2×10^4 to 4×10^4. When coefficient of drag was plotted against the Reynolds numbers for each object a similarity between curves was found. The three most aerodynamic objects 4, 5, and 6 had the most similar drag curves.

PACS numbers: 00001

I. OBJECTIVE

To become familiar with the effect of object' shape on its drag. This will be completed through an experiment utilizing different shaped objects subjected to flow within a wind tunnel. The drag forces caused by the varying shapes within the wind tunnel at varying flow speeds will be measured. Analysis of this data will aid in the understanding of the effect object' shape has on its drag.

II. BACKGROUND AND THEORY

In both Aerospace and Automotive industry, aerodynamics plays a critical role in vehicle design. Shapes and designs are optimized to obtain the lowest drag possible. One way of expressing drag is by using drag coefficients. The drag coefficient is a dimensionless number used to represent the overall effects of shape, inclination, and other flow conditions. The drag coefficient is defined as follows:

$$C_d = \frac{F_D}{\frac{1}{2}\rho U_\infty^2 A} \tag{1}$$

Where F_D is the drag force, ρ is the fluid density, U_∞ is the free stream velocity and A is the projected area of the object. Different shaped objects with the same Reynolds number and identical frontal areas can have very different drag forces and drag coefficients. Figure 1 compares the drag coefficients between different shaped objects with identical frontal areas. The Flat Plate has a noticeably greater coefficient of drag then the Bullet and Sphere.

III. PROCEDURE

Experiment 1 was conducted at California State University of Long Beach with the Engineering Technology Lab Wind Tunnel. The following procedures were used.

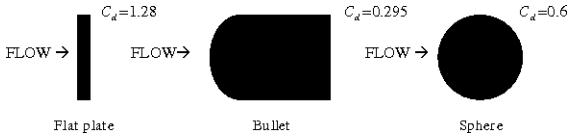

FIG. 1: Drag Coefficients of standard shapes

A. Part 1

A one-dimensional balance was used to calibrate the load cell within the Wind Tunnel. Weights varying from 0.6 to 6.6 lb were added and the output voltage of the load cell was measured. The calibration data is presented within the data section. The schematic setup can be seen in Figure 2.

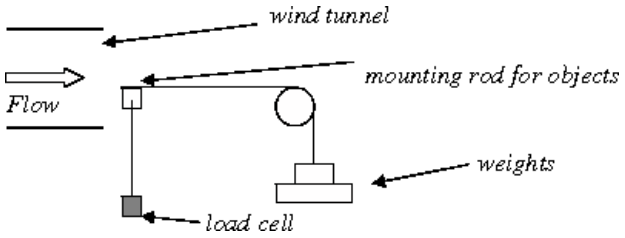

FIG. 2: Schematic Setup

B. Part 2

Six objects were attached one at a time to the mounting rod within the wind tunnel. Each object was subjected to different flow speeds, ranging from $11\frac{m}{s}$ to $22\frac{m}{s}$. At each flow speed, the voltage output from the load cell and the H_2O pressure drop from a pitot tube were recorded. During the experiment it was found that the pressure difference readings fluctuated considerably and as such, an average value was recorded.
The importance of the concept of blockage has to mentioned here. Blockage is defined as the ratio of the projected area

of the model divided by the total cross sectional area of the windtunnel. To obtain accurate results, this ratio should be less than 6%. Empirical data of the windtunnel suggests that we are below this margin. Figure 3 displays how the experiment was conducted.

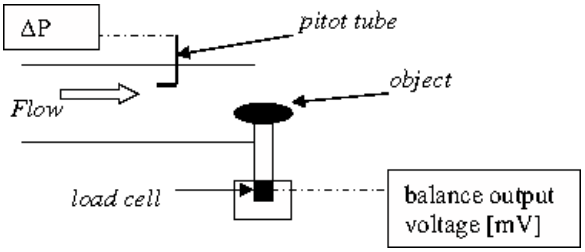

FIG. 3: Experimental Setup

C. Part 3

Measure and record the relevant object dimensions with a caliper. The test objects are displayed in figure 4, in the numeric order as they are addressed throughout this report.

IV. DATA

The original data sheet is attached to this report as Attachment No 1.

V. CALCULATIONS

The basic assumption used in all following calculations is that the working fluid, air, is an incompressible fluid. This is a reasonable assumption for low speeds such as those involved in this testing. Standard day atmospheric conditions of air are also used within these calculations.

TABLE I: Nomenclature, SLS Conditions

C_d	drag coefficient
F_D	drag force
ρ	air density
U_∞	free stream velocity
ν	kinematic viscosity
ΔP	pressure difference
V	output voltage
A	projected area
L	characteristic Length

A. Calibration

The output measurement of the load cell used in this experiment is voltage. A relationship must be found between this output voltage and the force. This relationship will allow us to calculate the drag force of the models within the windtunnel during testing. The process for collecting the calibration data is outlined in the procedures section . A plot of the data is shown in Figure 5.

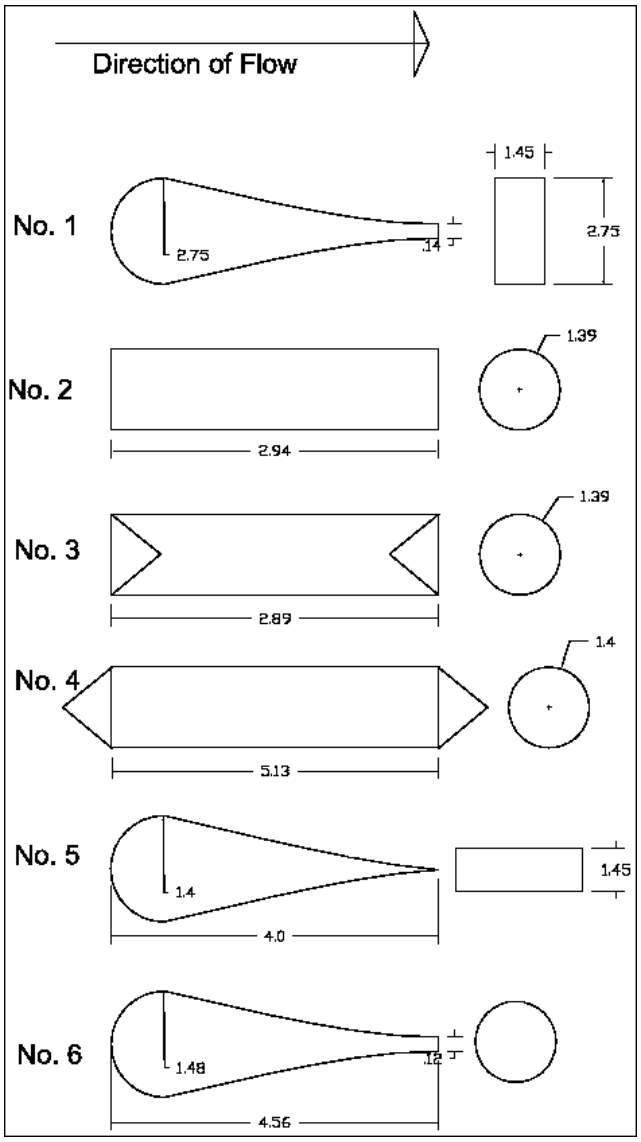

FIG. 4: Tested Objects, Dimensions: inch

From the output voltages recorded previously and this relationship the drag forces can be calculated for each object. However, the linear relationship $F_D = 1.77222x - 0.3663$ produces strange drag data, some drag coefficients go as high as 20, some are negative since due to a negative y intercept. Since there must have been an error in the calibration of the windtunnel, a more reasonable expression will be used in following charts and analysis: $F_D = 0.63x$. More on this in the discussion section.

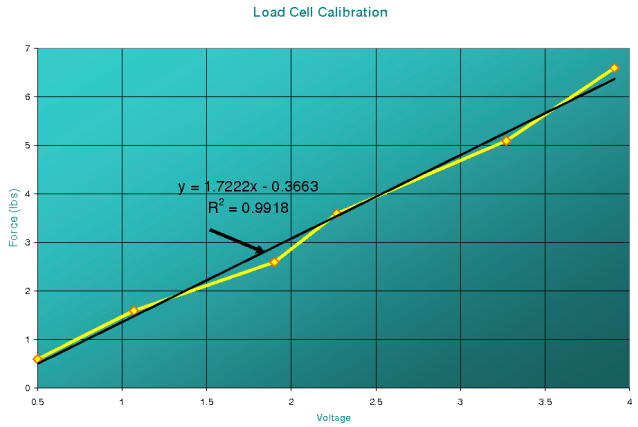

FIG. 5: Load Cell Calibration

B. Drag Coefficient

The recorded data for the experiment included ΔP readings with the units of $in\ H_2O$. This data had to be converted into a metric velocity unit, which is common and practical for use in later formulas. The following formulas were used for converting the ΔP readings.

$$U_\infty = 19.91 \times \sqrt{\Delta P} \tag{2}$$

After calculating the drag force with the linear relationship of volts and force and the free stream velocity (2), the drag coefficient can be found (1).

C. Reynolds Number

The Reynolds number is a measure of the ratio of inertia forces to viscous forces. Having found the free stream velocity earlier it is possible to calculate the Reynolds number for each condition using the following relationship:

$$Re_\infty = \frac{\rho U_\infty L}{\mu} = \frac{U_\infty L}{\nu} \tag{3}$$

D. Uncertainties

Uncertainties were analyzed for the velocities, Reynolds numbers, and drag coefficients. As expected, the force vs differential pressure plots were nearly linear. The uncertainties carried through to the drag coefficient uncertainties. The variables in the velocity calculations were differential pressures. The differential pressure display seemed to fluctuate during testing. It is encouraging that the resulting velocity standard deviations were very low. The uncertainties for the Reynolds's numbers and drag coefficients point to the differences in airflow around the objects. The uncertainties inherent to the measurement methods were as follows:

TABLE II: uncertainties

voltage reading	$\pm 0.005\ V$
pressure reading	$\pm 0.0005\ in\ H_2O$
measurements of length	$\pm 0.0005\ in$

A correlation coefficient (r) can be used to describe the strength of a linear relationship between two variables. This value was calculated for the linear function for force and measured output voltage: $r = 0.9918$ This value gives a high level of certainty for using this linear function to measure the drag force. With this level of certainty, this equation will be assumed to have no error.

TABLE III: Calculated Uncertainties

drag force	$\pm 0.0002\ lb$
ΔP	$\pm 0.00002\ psi$
free stream velocity	$\pm 0.004\ m/s$
Re	± 0.004

1. Sample Calculations

Using previous calculated uncertainties, the uncertainty of drag coefficient can be calculated:

$$C_d = f(F_D, U^2)$$

$$\Delta_{C_d} = \pm\{[\frac{F_D}{C_d}\frac{\partial C_d}{\partial F_D}\Delta_{F_D}]^2 + [\frac{U_\infty^2}{C_d}\frac{\partial C_d}{\partial U_\infty^2}\Delta_{U_\infty^2}]^2\}^{\frac{1}{2}} \approx 0.004$$

VI. TABLES AND GRAPHS

Attachment 2 shows the obtained results for the calculations completed to obtain the Coefficient of drag and Reynolds number for each object at each flow speed. Figure 6 and 7 show plots of Drag Coefficient versus Velocity and Drag Coefficient versus Reynolds Number, respectively.

VII. DISCUSSION OF RESULTS

The calculations show that for all objects, the drag forces increased as the free stream velocity and Reynolds number increased. The shapes of the six objects tested did have a major impact on the measured drag. By analyzing the results with the individual shapes it is easy to see that object that had the most aerodynamic shape also had the lowest drag. Object 4, 5 and 6 clearly have the most aerodynamic shapes as well as the lowest drag. It could possibly be the sharp edges and

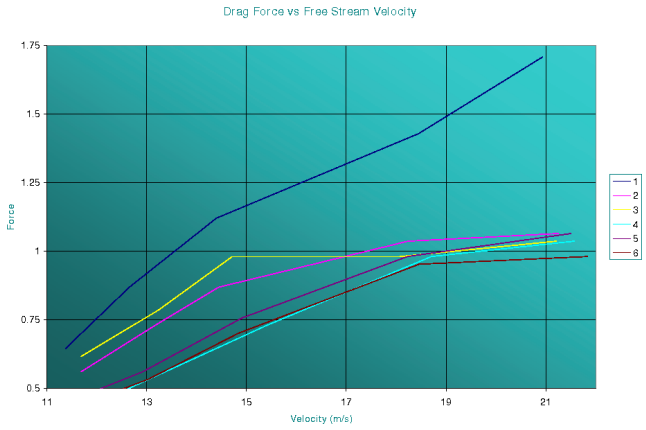

FIG. 6: Drag Coefficients vs Velocity

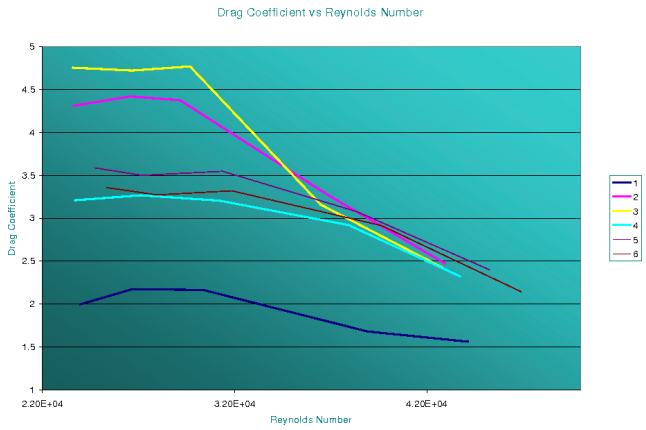

FIG. 7: Drag Coefficients vs Reynolds Nr

the frontal area of Object 1 that caused it to have the greatest measured drag. Objects $1-3$ do not have a single point of stagnation, but a whole area. Certainly, this is a source for additional drag, too.

The largest coefficient of drag values occurred at the low free stream velocities. Object 1 had the greatest cross sectional area as well as the lowest coefficient of drag values. Objects $2-6$ had similar areas while Object 3 had the highest calculated values of coefficient of drag. This is certainly due to its very unusual shape, which is subject to a large pressure differential. This would be expected because Object 3 looked the least aerodynamic. It is interesting to notice that Object 3's Drag force is above Objects 2's at lower velocities and below Object 2 at velocities greater than $17\frac{m}{s}$. Since shapes are similar, viscous drag is not the source of this. It seems that the pressure differential gets smaller as velocity increases.

Plotting the Reynolds numbers vs. coefficient of drag for each object showed similar curves. Note that the characteristic length of Object 1 is unlike all other objects not the length, but its width. It is clear to see that these values are closely related. So even though the calibration of the experiment might be incorrect and so are absolute drag values, the data nicely shows the relative differences between the shapes. For the range of values tested, the coefficient of drag decreases as the Reynolds number increases. Objects 4, 5 and 6 had the most similar slopes for this relationship. Object 1 had a much lower slope then the other objects, since its area can not really be compared with the other objects. Furthermore, it may be hypothesized that this difference in shape caused this unique behavior.

The calculated uncertainties and errors were within reasonable levels for the testing conducted. They provided reasonable accuracy for the analysis needed. One possible area of error that was not mentioned or considered within this report is the effects that temperature change on the measuring equipment. However, since even low variations in cryogenic windtunnel cause minimal effect, this can be neglected.

VIII. CONCLUSION AND RECOMMENDATIONS

Windtunnel testing was conducted in order to become more familiar with the relationship between an objects shape and its drag. Calibration of a load cell using known weights was first carried out. This lead to a linear relationship for accurately calculating objects drag forces within a windtunnel. This equation was found to have a high level of certainty (r=0.9918), even though it was ignored for this experiment. The flow speed velocity within the windtunnel was calculated using a pitot tube that measured pressure differences.

Six objects with similar sizes but different shapes were individually tested inside the windtunnel. Each object was subjected to five different free stream velocities (from $11\frac{m}{s}$ to $22\frac{m}{s}$) with drag forces measured using the load cell. Using the data recorded, the coefficient of drag and Reynolds number was calculated for each object. The data proved that object shape does play a large factor in drag.

The lesser aerodynamic shape (Object 3, 1, 2) resulted in drag forces more than double that of the object with the more ideal aerodynamic shape (Object 6). For the 3 Objects tested with similar projected areas, the objects with the most aerodynamic shapes had lower coefficient of drag and drag force values. Relationships between the coefficient of drag vs. Reynolds number curves and objects shape were also found.

The calibration of the facility is essential to make absolute predictions of the tested objects. However, since it was more important to understand the relative differences between shapes, the experiment was a success. Nevertheless, calibration has to be done more accurately for future experiments.

[1] Dr. Hamid Rahai, MAE 440 Aerodynamics Laboratory Experiments, California State University Long Beach, Spring 2007
[2] John J. Bertin, Aerodynamics for Engineers, 4th edition, 2002
[3] Personal notes